Autoionization Dynamics of Excited Collision Systems: Angular Dependence of the Electron and Ion Energy Spectra for $He^*(2^3S)+H$

A. Merz, M.-W. Ruf, and H. Hotop

Fachbereich Physik, Universität Kaiserslautern, W-6750 Kaiserslautern, Federal Republic of Germany

(Received 13 August 1992)

We present the first angle-dependent energy spectra for the basic autoionization process $He^*(2^3S)+H(1^2S)$ leading to Penning ionization ($\rightarrow He+H^++e^-$; PI) and associative ionization [$\rightarrow HeH^+(v^+,J^+)+e^-$; AI]. Our results include electron energy spectra for both reaction channels and the H^+-ion energy spectra for PI. The variation of the electron spectra with angle demonstrates the presence of substantial contributions from non-s-type electron partial waves, with the angle-dependent electron signals due to AI yielding clear information on the internal electron angular distribution of the autoionizing quasimolecule.

PACS numbers: 34.50.Gb, 33.70.−w, 34.50.Lf

The autoionization dynamics of collisional complexes is a lively topic of research [1–11] and the recent developments in laser cooling and trapping of atoms have created additional interest in ionization processes of excited atoms at low collision energies E_{rel} [3,4,12]. Besides studies of the velocity dependence of the ion production [3,10,11,13,14] and analyses of the ion angular distributions [7,8], high-resolution electron spectrometry of ionizing collision systems has proven especially fruitful in revealing details of the autoionization dynamics [1,2,4–6, 11,15–17] and in yielding direct information on the underlying interaction potentials [4,5,15–18]. One of the basic properties of the autoionizing collisional complex is its internal electron angular distribution, i.e., the angle-dependent electron intensity, as emitted in the frame of the autoionizing quasimolecule for specified internuclear distance R. Several authors [6,19–22] have addressed the problem of how to extract this property from electron angular distributions, measured with respect to the collision velocity axis. The experiments carried out at thermal collision energies [6,19,22–25] always involved an average over impact parameters and—with two exceptions [17,25]—dealt with the angular dependence of cross sections integrated over electron energy. Energy-integrated data, however, provide less information on the internal angular distribution than electron-energy-differential results, especially for attractive systems (with potential well depth large compared with the collisional energy) which tend to yield isotropic energy-integrated cross sections [19,22]. Previous work on spontaneous electron emission from slow atomic collisions at keV energies yielded detailed information on the charge cloud distribution and alignment of autoionizing *atomic* states, as derived from energy- and angular-resolved electron-ion-coincidence measurements [2].

In the present work we investigate one of the simplest autoionizing collision systems,

$$He^*(2^3S_1)+H(1^2S_{1/2}) \rightarrow \begin{cases} He(1^1S)+He^++e^- \ \text{(PI)}, & \text{(1a)} \\ HeH^+(v^+,J^+)+e^- \ \text{(AI)}. & \text{(1b)} \end{cases}$$

For some time, this reaction has been regarded as a model system, both experimentally and theoretically ([2,5, 15,16,26] and references in [16]). The good agreement between the high-resolution electron energy spectrum [16]—partially resolving the rovibronic structure due to $HeH^+(v^+,J^+)$ formation—and a quantum mechanical, optical potential calculation seemed to indicate that the ionization process is well described by the underlying theory [16]. The calculation involved accurate *ab initio* potentials for the real parts $V_*(R)$ and $V_+(R)$ of the He^*+H and $He+H^+$ systems, an adjusted imaginary part (autoionization width) $\Gamma(R)$ for the coupling of the entrance channel to the continuum, and the assumption that the heavy-particle angular momentum is conserved ($J^*=J^+$) in the electron emission process, implying isotropic electron emission (s wave only). Recent work on the rather similar, attractive system $He^*(2^3S)+Li(2^2S)$ revealed a substantial angular variation of the shape of the electron energy spectrum [5,17], which was attributed to angular momentum exchanges $|\Delta J|=|J^*-J^+|$ between the heavy-particle system and the emitted electron. A classical estimate based on recoil arguments yielded $|\Delta J_{max}|\approx 4\hbar$, compatible with the significant angle-dependent changes of the spectral shapes [17]. A similar consideration for He^*+H results in $|\Delta J|\lesssim\hbar$, supporting the idea of negligible angular momentum exchange in this system. It has to be noted, however, that the width $\Gamma(R)$, adjusted for $He^*(2^3S)+H$ [15,16], exhibits a much stronger decrease towards larger R than theoretical *ab initio* widths [5,26]. This discrepancy and the He^*+Li results provided the motivation to carry out the first angular-dependent study of the $He^*(2^3S)+H$ system. The obtained results demonstrate substantial anisotropy in the angle-dependent spectra and provide for the first time direct information on the internal electron angular distribution.

Our experimental setup, shown in Fig. 1, involves crossed atomic beams and two double hemispherical condensers for electron and ion detection. The metastable

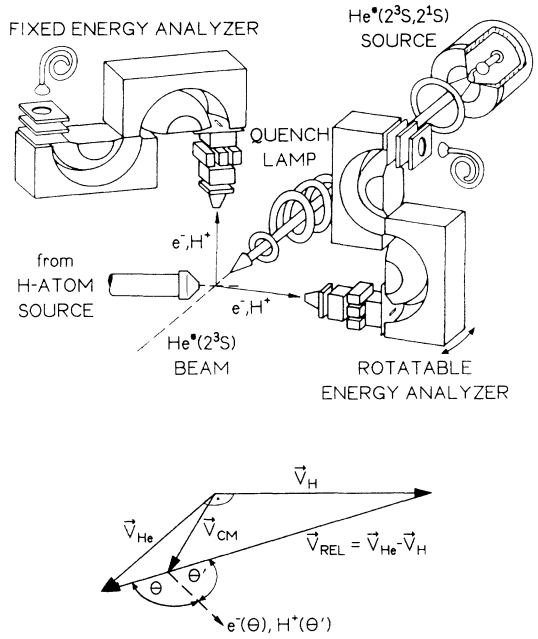

FIG. 1. Semischematic illustration of the crossed-beam apparatus for the study of the angular dependence of the electron and ion energy spectra due to $He^*(2^3S)+H(1^2S)$ collisions. The velocity diagram involves the respective average velocities.

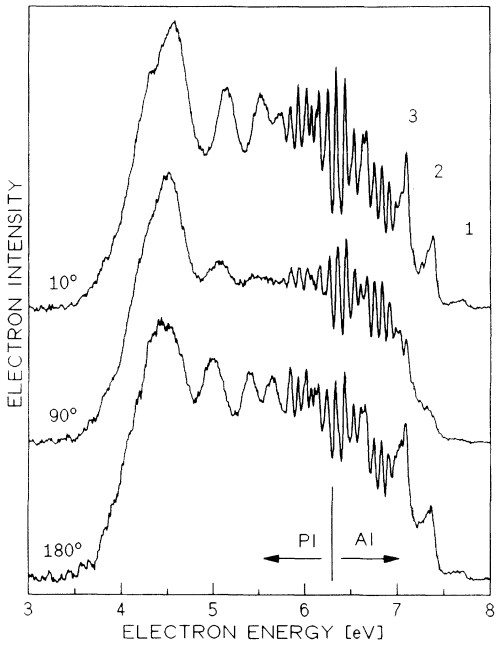

FIG. 2. Energy spectra of electrons from $He^*(2^3S)+H(1^2S)$ collisions, as observed at the detection angles $\Theta=10°$, 90°, and 180°. The dotted lines labeled 1, 2, and 3 mark the onsets for the formation of $HeH^+(v^+,J^+=0)$ ions for $v^+=1$, 2, and 3. The three spectra have a common intensity scale, which is proportional to the cross section.

helium atoms are produced in a differentially pumped cold-cathode dc discharge [18]. $He^*(2^1S)$ atoms are removed from the beam to an amount of less than 0.5% of their original contribution ($2^3S/2^1S=8/1$) via optical pumping, using the irradiation from an air-cooled helium dc discharge surrounding the He beam [16]. The resulting pure $He^*(2^3S)$ beam can be monitored by a Faraday cup and has an intensity of 1.5×10^{15} atoms/ssr. The average metastable velocity is $\bar{v}_{He}=1750$ m/s with a width of $\Delta v/\bar{v}_{He}\simeq30\%$. The atomic hydrogen beam is produced in an air-cooled microwave discharge outside the vacuum chamber and is guided to the reaction zone by a PTFE-covered stainless-steel tube, yielding an effective density ratio of $n(H)/n(H_2)\approx0.3$. The velocity distribution of the H atoms was not measured, but can be assumed to be a Maxwell distribution for an effusive quasibeam ($T=300$ K, $\bar{v}_H=2500$ m/s) [16]; the average relative collision energy is $\bar{E}_{rel}=50$ meV. One of the two spectrometers detects charged particles at 90° with respect to both atomic beams and serves as a monitor to allow the determination of angle-dependent, energy-integrated cross sections; its detection geometry corresponds to the one always used in previous work. The second spectrometer is rotatable to detect electrons (ions) in the collision plane spanned by the two atomic beams. Both detectors are operated at the fixed transmission energy of 4.8 eV leading to an effective resolution of about 30 meV. The electron energy spectra contain a non-negligible contribution due to Penning ionization of ground-state molecular hydrogen (below 4.5 eV) and a minor contribution due to the reaction $He^*(2^3S)+HF$ (below 3.8 eV). The electron spectra for both processes were separately measured and properly subtracted together with a small and almost constant background. The energy scale is calibrated accurately (±8 meV) by comparison with the well-known spectra for $He^*(2^3S)+H_2$ [27], simultaneously measured. The results are corrected for the energy dependence of the spectrometer transmission [28]. The overall angular resolution of the experiment is limited by the angular and velocity widths of the effusive H atom beam and estimated to be better than $\pm30°$.

Figure 2 shows three out of six electron energy spectra measured at the detection angles $\Theta=10°$, 30°, 90°, 120°, 150°, and 180°. The angle Θ refers to the relative velocity vector $\mathbf{v}_{rel}\equiv\mathbf{v}_{He}-\mathbf{v}_H$, with $\Theta=180°$ labeling the backward direction of electron emission from the He atom in the center-of-mass frame (see Fig. 1). All the spectra show Airy-type interference patterns at energies $\epsilon\lesssim5.8$ eV, associated with two coalescent points of stationary phase [4,5,15,16,22,29] and in this case due to a well-characterized minimum in the electron energy function $\epsilon(R)=V_*(R)-V_+(R)$ [5,15,16]. Furthermore, one observes distinct structure due to the formation of quasibound rovibrational levels of $HeH^+(v^+,J^+)$ with high J^+ around 25 in the range $5.8\lesssim\epsilon\lesssim6.27$ eV [16], and partially resolved rovibronic structure due to the formation of truly bound $HeH^+(v^+,J^+)$ levels at electron en-

ergies $\epsilon > 6.27$ eV [16] [i.e., $\epsilon > E_0 + \bar{E}_{rel}$ with E_0 equal to the $He^*(2^3S)$ energy minus the ionization energy of $H(1^2S)$]. We emphasize the substantial differences between the three spectra in Fig. 2, which are observed in spite of the limited angular resolution of our experiment: The Airy-type and quasibound structures are more strongly modulated in the forward ($\Theta = 10°$) and in the backward ($\Theta = 180°$) direction than at $\Theta = 90°$; the present $\Theta = 90°$ data—with almost identical results obtained from both the rotatable and the fixed monitor detector—are in essential (but not perfect) agreement with the previous work [15,16] (a detailed comparison and critical discussion will be presented elsewhere). Similar to the variation first observed for $He^*(2^3S) + Li$ [17], the Airy interference pattern is found to smoothly shift towards lower energies, when going from $\Theta = 10°$ to 180°, most notably so for the three supernumerary peaks, observed at about 5.0, 5.4, and 5.65 eV, respectively, for $\Theta = 180°$.

Perhaps the most striking result is the strong intensity variation in the energy ranges immediately below the onsets for $HeH^+(v^+ = 1\text{-}3, J^+ \geq 0)$ formation, indicated by dotted lines in Fig. 2. In the spectra taken at $\Theta = 10°$ and 180°, a steep rise is observed towards a maximum located within 0.1 eV of the onset, whereas at $\Theta = 90°$ the intensity rises gradually towards lower energies; the latter behavior closely resembles the calculated AI intensities, as discussed previously [16]. The data at $\Theta = 10°$ and 180° therefore signal a strong enhancement for AI into low J^+ rotational levels as compared to $\Theta = 90°$. Inspection of the calculated rovibrational AI cross sections and energy levels [16] shows that the intensity variation in the 0.1-eV interval below the $v^+ = 1$ and 2 onsets can be directly correlated with the angular-dependent cross sections for the population of the respective $J^+ = 0\text{-}5$ rotational levels. Low J^+ final states originate from low J^* initial angular momenta, i.e., are due to collisions with small impact parameter; $HeH^+(v^+, J^+)$ ions with low v^+ and J^+ can only be formed if the excited quasimolecules penetrate to small internuclear distances [$R = (2.2\text{-}2.4)a_0$ [16]]. Classical trajectory calculations show that the orientation of autoionizing quasimolecules with $J^* = 0\text{-}5$ and $R \approx 2.3a_0$ is confined to a rather narrow angular range of about $\pm 25°$ around the relative velocity direction.

The inherent orientation of those autoionizing molecules which are associated with the energy-resolved detection of low J^+ AI products allows for the first time a qualitative reading of the internal electron angular distribution directly from the corresponding Θ-dependent electron intensities. From an inspection of the $v^+ = 1$, 2, and 3 onsets in our six measured spectra we conclude that the internal angular distribution exhibits similar maxima in the backward as well as in the forward direction; they exceed the minimum around $\Theta = 90°$ by at least a factor of 2–3. To our knowledge such direct experimental information on the internal electron angular distribution has not been previously reported. We note that recent *ab initio* calculations of the internal angular distribution for $He^*(2^3S) + Li$ [30] indicate a maximum in the forward direction (i.e., in the direction of the vector pointing from He^* to the target atom), which can be attributed to the focusing action of the Coulomb potential centered on the ionized target atom. We also mention that calculations of Hertzner [31] on the internal electron angular distribution for the repulsive system $He^*(2^1S) + Ar$ yielded maxima both in the forward and in the backward directions.

The orientational selectivity associated with near-zero-impact-parameter collisions, discussed above for the AI signals at low J^+, is present for all the kinetic energies of the thermal distribution. Although dependent on collision energy, the near-orbiting trajectories (J^* around 25 at $E_{rel} \approx 50$ meV), which lead to quasibound ion states ($J^+ = 23\text{-}27$ for the 5.8–6.1-eV range) by electron emission close to $2.4a_0$, also retain significant orientational selectivity: Electron emission occurs with molecular orientations opposite to those for low J^*, but again almost parallel to $\mathbf{v}_{rel}$. Similar to the AI signals at low J^+, the angular variation of the modulation strength of the structure in the 5.8–6.1-eV range indicates significantly larger contributions from the highest partial waves ($J^* = 23\text{-}27$) in the forward and backward directions than into angles around $\Theta = 90°$. With regard to the angular variation of the Airy oscillation structure ($\epsilon \lesssim 5.8$ eV), we note that this part of the electron spectrum is due to electron emission over a large range of internuclear distances, preventing the direct interpretation of the data in terms of an internal angular distribution, which is expected to be R dependent. As observed previously for other attractive PI systems [19,22], the energy-integrated electron intensities depend only weakly on angle; a satisfactory fit to our data points is obtained with the expression $P(\Theta) = \sum_{n=0}^{2} a_{2n} \cos 2n\Theta$ ($a_0 = 1$, $a_2 = 0.080$, $a_4 = 0.126$), indicating symmetry around $\Theta = 90°$.

We now briefly discuss the angular dependence of the H^+ energy spectra, corresponding to Penning ionization at electron energies $\lesssim 5.7$ eV (Fig. 3). The $\Theta' = 0°$ spectrum corresponds to forward scattering of the H^+ ions [i.e., along the $H(1s)$ direction in the center-of-mass (CM) frame; see Fig. 1]. Apart from an angle-dependent energy shift due to the influence of the CM motion which is expected to be largest for $\Theta' \approx 107°$ (H^+ emission in the direction of the CM velocity), the spectra have similar shapes in the Θ' range 0°–90° with an Airy interference structure similar to that observed in the electron spectrum at $\Theta = 90°$. Towards backward angles ($\Theta' > 90°$) additional structure emerges in the main Airy peak, which can be attributed to the so-called "fast oscillations" [4,26] due to the interference of incoming and outgoing heavy-particle waves. Their presence indicates that only a restricted number of angular momenta contribute, as expected for backward scattering (contribu-

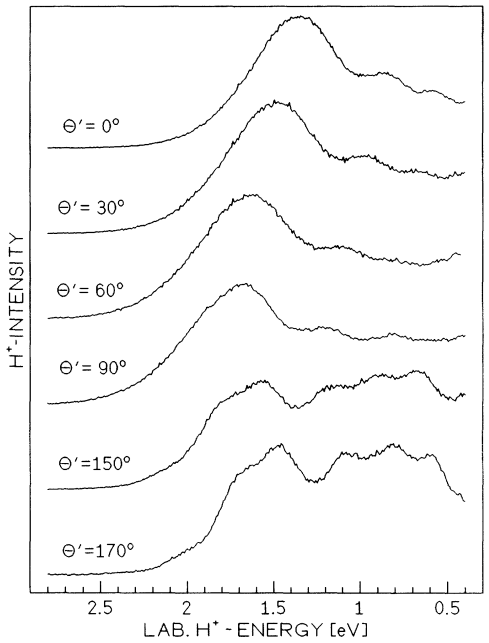

FIG. 3. Energy spectra of H^+ ions due to Penning ionization in $He^*(2^3S)+H(1^2S)$ collisions, as observed in the laboratory H^+ energy range 0.4–2.8 eV at the six given detection angles Θ'. The spectra are normalized to equal height at the respective maxima.

tions from low J^*/J^+, accompanied by selected high J^*/J^+ orbiting trajectories leading to Θ' around 180°). The energy-integrated, angle-dependent H^+-ion cross section peaks at $\Theta'=0$, similar to previous results for $He^*(2^1S)+H$ [7] and $Ne^*(^3P_2)+H$ [8]. Beyond a minimum near $\Theta'=90°$ we observe an increase towards the backward direction. To our knowledge, such a backward peak has not been previously reported for Penning ions. It is likely that this backward peak is in part due to near-orbiting trajectories.

The data presented in this paper provide the first angle-dependent electron and ion energy spectra for the basic autoionization system $He^*(2^3S)+H$. We have shown that several features of the observed spectra allow direct conclusions to be drawn on fundamental properties of the autoionizing molecule (such as the internal electron angular distribution) and thereby to obtain deep insight into the autoionization dynamics of small collisional complexes. Our detailed experimental results will present a sensitive test of *ab initio* theory. We note that calculations on the autoionization amplitudes [30] are in progress; they will shed more light on the role of non-*s*-type electron partial waves and the corresponding anisotropic electron angular distributions.

We acknowledge support of this work by the Deutsche Forschungsgemeinschaft through Sonderforschungsbereich 91. We thank Professor W. Meyer for the communication of unpublished results and useful discussions and Dr. A. Hertzner for providing a copy of his dissertation.

[1] H. Morgner, Comments At. Mol. Phys. **21**, 195 (1988).
[2] A. Niehaus, Phys. Rep. **186**, 149 (1990).
[3] J. Weiner, F. Masnou-Seeuws, and A. Giusti-Suzor, Adv. At. Mol. Phys. **26**, 209 (1990).
[4] M. W. Müller *et al.*, Phys. Rev. Lett. **59**, 2279 (1987); M. W. Müller *et al.*, Z. Phys. D **21**, 89 (1991).
[5] A. Merz *et al.*, Chem. Phys. **145**, 219 (1990).
[6] K. Mitsuke, K. Kusafuka, and K. Ohno, J. Phys. Chem. **93**, 3062 (1989).
[7] A. Khan, H. R. Siddiqui, and P. E. Siska, J. Chem. Phys. **94**, 2588 (1991).
[8] A. Khan, H. R. Siddiqui, and P. E. Siska, J. Chem. Phys. **95**, 3371 (1991).
[9] J. P. J. Driessen *et al.*, Phys. Rev. A **42**, 4058 (1990).
[10] X. Urbain *et al.*, Phys. Rev. Lett. **66**, 1685 (1991); X. Urbain, A. Cornet, and J. Jureta, J. Phys. B **25**, L189 (1992).
[11] B. Brunetti and F. Vecchiocattivi, in "Current Topics in Ion Chemistry and Physics," edited by C. Y. Ng (Wiley, New York, to be published).
[12] P. D. Lett *et al.*, Phys. Rev. Lett. **67**, 2139 (1991); P. S. Julienne and R. Heather, Phys. Rev. Lett. **67**, 2135 (1991).
[13] J. Fort *et al.*, Phys. Rev. A **18**, 2063 (1978).
[14] R. H. Neynaber and S. Y. Tang, J. Chem. Phys. **69**, 4851 (1978).
[15] H. Morgner and A. Niehaus, J. Phys. B **12**, 1805 (1979).
[16] H. Waibel, M.-W. Ruf, and H. Hotop, Z. Phys. D **9**, 191 (1988).
[17] A. Merz *et al.*, Chem. Phys. Lett. **160**, 377 (1989).
[18] M.-W. Ruf, A. J. Yencha, and H. Hotop, Z. Phys. D **5**, 9 (1987).
[19] T. Ebding and A. Niehaus, Z. Phys. **270**, 43 (1974).
[20] D. A. Micha and H. Nakamura, Phys. Rev. A **11**, 1988 (1975).
[21] V. Hoffmann and H. Morgner, J. Phys. B **12**, 2857 (1979).
[22] A. Niehaus, Adv. Chem. Phys. **45**, 399 (1981).
[23] H. Hotop and A. Niehaus, Chem. Phys. Lett. **8**, 497 (1971).
[24] A. Le Nadan *et al.*, J. Phys. (Paris) **43**, 1607 (1982).
[25] A. Hertzner *et al.*, in *Proceedings of the Fourteenth International Conference on the Physics of Electronic and Atomic Collisions, Palo Alto, 1985, Abstracts of Contributed Papers,* edited by M. J. Coggiola, D. L. Huestis, and R. P. Saxon (North-Holland, Amsterdam, 1985).
[26] A. P. Hickman, A. D. Isaacson, and W. H. Miller, J. Chem. Phys. **66**, 1483 (1977).
[27] T. Bregel *et al.*, Z. Phys. D **13**, 51 (1989).
[28] J. Lorenzen *et al.*, Z. Phys. A **310**, 141 (1983).
[29] W. H. Miller, J. Chem. Phys. **52**, 3563 (1970).
[30] W. Meyer and M. Movre (to be published).
[31] A. Hertzner, dissertation, University of Witten, 1990 (unpublished).